# IC-Processed Electrostatic Micro-motors

Long-Sheng Fan, Yu-Chong Tai, and Richard S. Muller

Berkeley Sensor and Actuator Center
An NSF/Industry/University Cooperative Research Center
Department of EECS and the Electronics Research Laboratory
University of California, Berkeley CA 94720

## ABSTRACT

We describe the design, fabrication, and operation of several micro-motors that have been produced using integrated-circuit processing [3]. Both rotors and stators for these motors, which are driven by electrostatic forces, are formed from 1.0-1.5 μm-thick polycrystalline silicon. The diameters of the rotors in the motors we have tested are between 60 and 120 μm. Motors with several friction-reducing designs have been fabricated using phosphosilicate glass (PSG) as a sacrificial material [4,5] and either one, or three polysilicon depositions.

## INTRODUCTION

Recent publications have discussed possible designs for micro-motors [1,2] based on electrostatic-drive principles. Using technology derived from IC manufacturing processes, we have built and tested several electrostatically driven rotating motors and driven them both in stepwise fashion and through continuous revolutions. Included among the motors are structures with 4 and 8 rotor poles and 6, 12, and 24 stator poles. Typical gaps between the rotors and stators in this first realization of operating micro-motors are 2 μm or greater. The technology for the motors, which have rotors that turn on stationary axles fixed to the silicon substrate, is based upon the processes described in [4, 5].

Design has been based on many assumptions because fundamental parameters and mechanical behavior at the micrometer scale are largely unknown at this time. Extensive research is now underway in our laboratory to determine mechanical and electrical behavior for these very small structures. We describe here the results of initial tests of the motors as well as some of the design ideas that we have incorporated in them. Separate sections of this paper are devoted first to discussion of the stepping motors, and second to discussion of the synchronous motors.

## STEPPING MOTORS

To design stepping motors for micropositioning, large starting torque, small frictional force, and fine angle resolution are desirable. Means to optimize these characteristics in micro-motors have been explored in our design. Figure 1 shows the top view and cross sectional view of a stepping motor that implements these features.

*Starting Torque:* The design of a rotating motor begins with an estimation of the torque exerted by the electric field. This can be expressed in terms of the derivative of the stored energy which, for a given bias $V$ between rotor and stator, is conveniently represented as $1/2\,C\,V^2$, where C represents the capacitance across the driving electrodes that have voltage V across them. To find the rotor torque $T$, we take the derivative with respect to the rotor angle θ.

$$T(\theta) = \frac{1}{2} V^2 \frac{\partial C(\theta)}{\partial \theta} \tag{1}$$

Torque values are of the order of pNm for voltages of order 100V and typical micro-motor dimensions. The angular dependence of this torque, which must overcome frictional restraint in order to cause the motor to rotate, is being studied in terms of electrostatic field plots such as the one shown in Fig. 2. The field-mapping program for Fig. 2 is a two-dimensional approximation. The regions of high equipotential-line density in Fig. 2 indicate locations of high electric fields. The effects of electrostatic drive are to maximize the field energy by aligning the rotor poles to the "active" stator poles. The rotor and stator in Fig. 2 are designed so that the next-to-be activated pole pair approximately aligns to the maximum torque position after each step, assuring a large starting torque for the next step.

Figure 4 shows bias and phasing scheme of these stepping motors. The size of the step for the motor is a function of the number of stators $n_s$ and rotors $n_r$. Its size Θ in radians is given by:

$$\Theta = 2\pi\left(\frac{1}{n_s} - \frac{1}{n_r}\right) \tag{2}$$

We only need six stator poles for a twenty-four-step angular resolution.

*Friction Reduction:* By designing the motors so that the plane of the rotor is slightly lower (typically 0.5 μm) than the plane of the stator, the electrical field will have a component perpendicular to the substrate which will give rise to a force that tends to lift the rotor from this surface and thus to reduce friction. The purpose of this levitation force is not to overcome gravitational force (the rotor has a mass measured in tens of nanograms), but rather to overcome electrical attraction of the rotor to the substrate.

Another technique to reduce friction is to provide bushings to support the rotor. Friction-reducing bushings have been incorporated in several of the motors. In one design, hemispherical bushings extend from the under-surface of the rotor to provide a small-area contact with the substrate as shown in figure 3. To make the bushings, circular holes are patterned in the resist covering the sacrificial-oxide layer [4,5] and this layer is then isotropically etched before depositing polysilicon to form the rotor. The resultant extended hemispheres of polysilicon reduce friction between the two surfaces.

Yet another approach to reducing friction between the surfaces has been to use silicon nitride as the hub material in several



CH2528-8/88/0000-0666 $1.00 © 1988 IEEE

of the stepping-motor designs. Our measurements have shown a smaller coefficient of friction to characterize silicon nitride in contact with polycrystalline silicon than is the case with two layers of polycrystalline silicon. We have therefore fabricated the stepping micro-motors using silicon nitride as the hub material.

### Fabrication and Test

The stepping motors have been made using a process similar to that described for making pin joints in references 4 and 5. For the micro-motors, however, silicon nitride is deposited in place of the second layer of polycrystalline silicon, and a silicon nitride/silicon dioxide composite layer is used for electrical isolation. Figures 5 and 6 show a stepping-motor with six stator poles and eight rotor poles; from Eq. (2), it will rotate with 15° steps. The polysilicon rotor is 60 μm in diameter and 1 μm-thick. The silicon-nitride hub is 1 μm-thick, and a 2-μm-wide lateral air gap separates rotor and stator. A silicon-nitride axle and four polysilicon-hemispherical bushings (2.0 μm in diameter) are used to reduce friction between the rotor and its supports. The polysilicon bushings, which reduce the contact area for the rotor, are built over a thin layer of silicon dioxide (500 nm), covered by silicon nitride (1 μm). This composite layer and bushing have also been designed to increase electrical isolation between the rotor and the substrate.

At this time, these motors have been moved with manually switched voltages. They have been tested at manual-switching rates of 12 rpm, and require starting voltages of roughly 120 V from stator to stator. Using Eq. (1), we estimate, therefore, that the frictional forces are in the tens of nN range.

## SYNCHRONOUS MOTOR

Figure 7 shows the top view of a synchronous motor having 12 stators and a 4-pole rotor so that it will function basically as a three-phase motor. Figure 8 shows the cross section along line AA' in Fig. 7 and makes apparent several friction-reducing schemes of the design. First, the rotor is supported by a flanged hub [4] that shortens the lever arm to the force point on the shaft. Second, both the stator and rotor are designed as coplanar structures to minimize the electrostatic force toward the substrate. Third, a ground plane is designed underneath both the rotor and the stator which is meant to have the same voltage as the rotor, thereby eliminating vertical electrostatic force. The ability to change both the ground-plane voltage and that of the stator provides an extra level of control for this motor design. Also apparent in Fig. 8 are silicon-nitride spacers at the vertical ends of the rotor and stator. The spacers interfacing with the hub act as solid lubricants to reduce friction and to provide wear protection for the rotor.

### Fabrication and Test

In the motor shown in Fig. 9, the rotor diameter is 120 μm, and the gap between the stator and the rotor is 4 μm. Figure 10 shows a similar but smaller motor with a 24-pole stator and a 8-pole rotor. The diameter of the rotor is 60 μm, and the stator-rotor gap is 2 μm. The motors in Figs. 9 and 10 both have cross sections as shown in Fig. 8, and are fabricated with a three-layer-polysilicon process.

To make the motors, the starting wafers are first covered with two insulating layers: a film of thermally grown silicon dioxide (300 nm) and a 1 μm overlay layer of silicon nitride. The first layer of polysilicon( 300 nm) is deposited and patterned to provides a grounding plate for the rotor. A 2.2 μm phosphosilicate glass(PSG) is then deposited to be the sacrificial layer[4,5]. After the anchor opening in the PSG, a second layer of polysilicon(1.5 μm) is deposited, thermally oxidized( 100 nm polysilicon dioxide), and patterned to form both the stator and rotor. A 340-nm film of silicon nitride is then deposited as the spacer material. Anisotropic reactive-ion-etch (RIE) of the nitride then forms the spacers. Flange opening is done by PSG wet etching, followed by deposition of a second layer of sacrificial PSG( 700 nm) to refill the rotor undercut. The hub anchor is then opened, followed by the deposition and patterning of the third layer of polysilicon( 1.5 μm). Sacrificial PSG etch in buffered HF finishes the process.

The synchronous motors have been tested in air under two drive conditions. First, the motors were tested with only one pair of the stators and the rotor biased as shown in Fig. 11. The rotor is grounded and voltage is applied to two stators across a diameter of the motor. The remaining stators are unconnected. Under these bias conditions, stepwise rotations have taken place at voltages ranging from 100 to 400 V. However, corona, or even electrical breakdown of air, has sometimes occurred at biases above 300V. Since the minimum distance between stator and rotor, or stator and ground plane, is about 2 μm, electric fields as high as $1.5\times10^{8}\,\mathrm{Vm}^{-1}$ can, therefore, be imposed without causing breakdown.

A second bias arrangement under which the motors have been tested makes use of three-phase signals as shown in Fig. 12. Under the 3-phase bias condition, motors of the type shown in Fig. 9 were set into continuous rotation and observed using a video camera. Using a 200 V drive voltage, the motor rotation is about 50 rpm, at 350 V, the maximum rotation is about 500 rpm.

## CONCLUSIONS

Electrical drive of rotating *IC*-fabricated micromechanisms has been demonstrated with examples of stepping and three-phase synchronous drive micro-motors described. Design features to minimize friction and to maximize torque in micro-motors are discussed. Typical drive voltages for present designs exceed 100 V. Manually switched motors have tested at speeds up to 12 rpm. Synchronous motors have been driven at speeds to 500 rpm. Experimental evaluation is continuing aimed mainly at understanding frictional effects.

*Acknowledgements* We thank Profs. D.J. Angelakos, R.M. White, and Paul T. Yang for valuable discussion, and K. Voros, R. Hamilton, D. Giandomenico and the staff of the Berkeley Microfabrication Laboratory for assistance in processing.

## REFERENCES

[1] W.S. Trimmer and K.J. Gabriel, "Design Considerations for a Practical Electrostatic Micromotor," *Sensors and Actuators*, 11, pp. 189-206, (March, 1987).

[2] S.F. Bart, T.A. Lober, R.T. Howe, J. H. Lang, and M.F. Schlecht, "Design Considerations for Microfabricated Electric Actuators," *Sensors and Actuators*, 14, pp. 269-292 (July, 1988).

[3] *Patent Pending.*

[4] R.S. Muller, L-S. Fan, and Y-C. Tai, "Micromechanical Elements and Methods for Their Fabrication," U.S. Patent 4,740,410, issued to the Regents of the University of California, April 26, 1988.

[5] L-S. Fan, Y-C. Tai, and R.S. Muller, "Integrated Movable Micromechanical Structures for Sensors and Actuators," *IEEE Trans. Electr. Devices*, ED-35, pp. 724-730, (June, 1988).

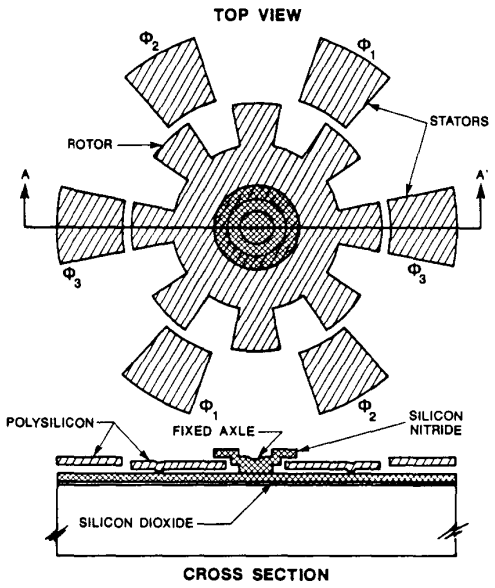


Figure 1 Top view and cross section of a stepping micromotor.

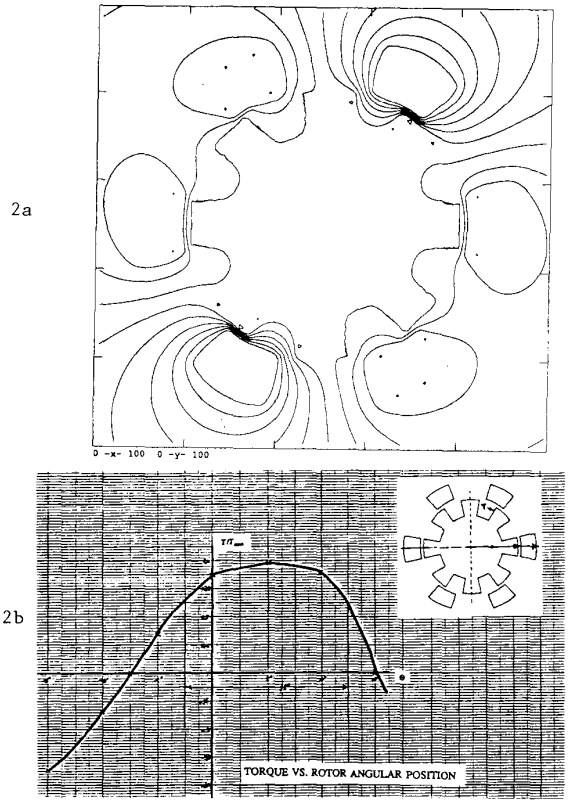


Figure 2 (a) Equipotential lines corresponding to a symmetrical biasing scheme from a two-dimensional simulation. (b) Torque versus rotor angular position from two-dimensional simulations.

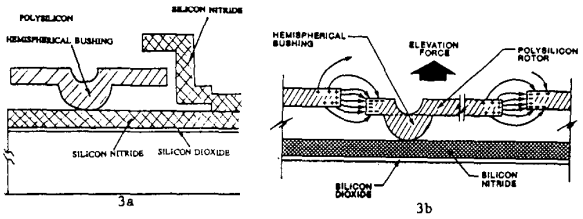


Figure 3 (a) Silicon-nitride axle and hemispherical bushing. The bushing provides a small-area contact with silicon nitride layer on substrate. (b) Levitation force to overcome substrate attraction.

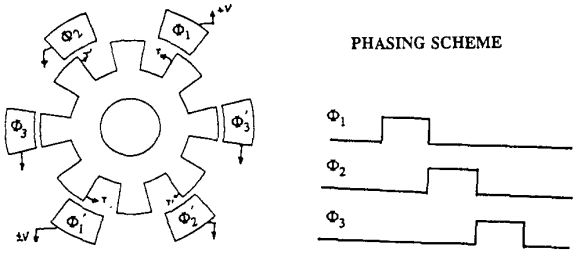


Figure 4 Biasing and phasing scheme of a stepping motor.

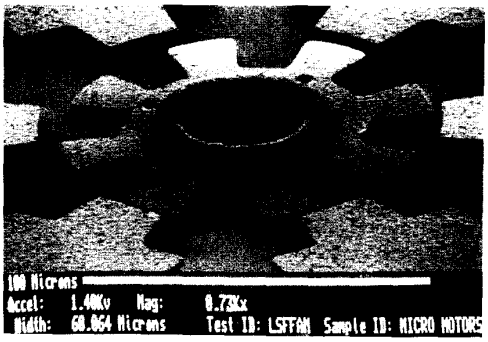


Figure 5 SEM photograph of a twenty-four-step stepping micromotor. The gap between the stator and rotor is 2 μm.

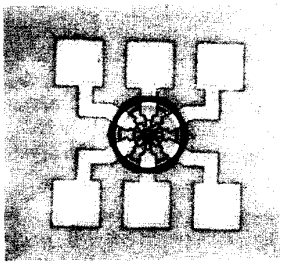

Figure 6 Photograph of the same motor in figure 5. Six contact pads are connected to the six stator poles.

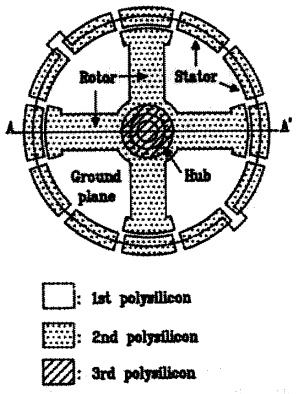


Figure 7 Top view of a synchronous motor.

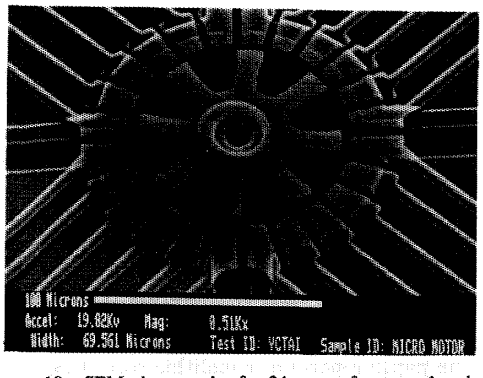


Figure 10 SEM photograph of a 24-stator, 8-rotor-pole micro motor. The gap between the stator and rotor is 4 μm.

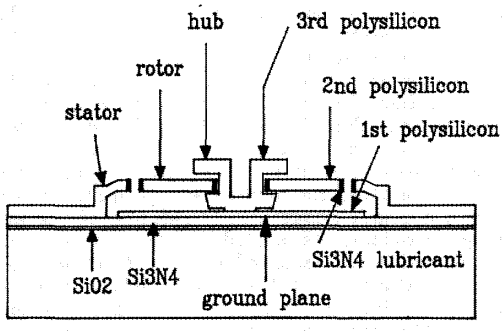


Figure 8 Cross section of line AA' in Fig. 1.

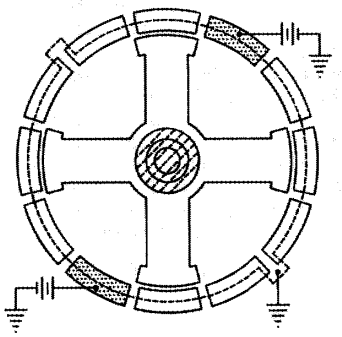

Figure 11 Stator-pair drive configuration. Only a pair of the stators are biased and the ground plane is grounded.

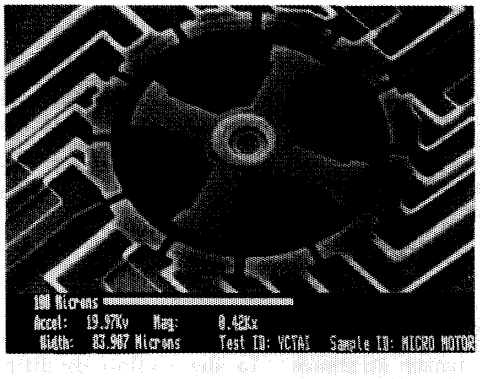


Figure 9 SEM photograph of a 12-stator, 4-rotor-pole micro motor. The gap between the stator and rotor is 6 μm.

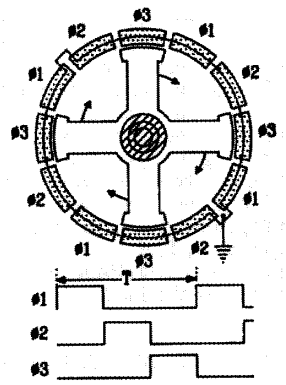


Figure 12 Three-phase drive configuration. All the stators are connected into three-phase scheme and the ground plane is grounded.